NUMERICAL MODELING OF DYNAMIC STALL IN A VERTICAL AXIS WIND TURBINE

Abdelouhed AYACHI AMAR[1], Amar BERKACHE[2], Salah AMROUNE[2,3,*]
Belkheir NOURA[4], Abdellah BOUMEHANI[5]
[1,4,5]FIMA, Laboratory university of Khemis Miliana ALGERIA.
[2]University Mohamed Boudiaf Msila ALGERIA
amar.berkache@univ-msila.dz
[3]LSSM, Laboratoire de Matériaux et Mécanique des Structures (LMMS), Université de M'sila. Algérie.
salah.amroune@univ-msila.dz

***ABSTRACT**: In this paper, a detailed numerical analysis of the effect of dynamic stall on the aerodynamic performance of a Darrieus H three-bladed vertical axis wind turbine is performed. To do this a series of simulations based on the Reynolds averaged Navier–Stokes (RANS).with turbulence modeling by the k-ω SST model is used. In order to quantify the influence of the dynamic stall on the aerodynamic performance of the rotor, the characteristics of the flow field around the rotor in different configurations are studied. For different velocity ratio values, dynamic magnitudes such as torque and rotor power are presented and analyzed. Also, two parameters are carefully studied: the mesh resolution and the size of the time step. In the analysis, it seems that these parameters affect the accuracy of the results. The numerical results show that dynamic stalling directly affects energy production. The results obtained show that the blades performance decreases when the profile is stalled, it is therefore important to design wind turbines that operate within the limit of dynamic stall. Finally, the numerical results of the power coefficient of the rotor are compared with the experimental data from the bibliography. An error of 8% is observed in this comparison.*

***KEYWORDS**: Wind turbine; VAWT Darrieus; rotor H; dynamic stall;CFD; RANS*

1 INTRODUCTION

The Due to the intensive efforts in recent years, the conversion of wind energy has become a reliable source of generating electricity. This energy sector is currently expanding. The use of the Darrieus vertical axis wind turbine seems beneficial for low wind speeds. The Research on these wind turbines (VAWT) shows that they have several advantages over horizontal axis wind turbines (HAWT). These wind turbines are extremely quiet, due to their particular design in which the blades do not create the usual noise of horizontal axis wind turbines. These wind turbines also have the advantage of being independent of the wind direction. However, it suffers from a low efficiency compared to horizontal axis wind turbines.

The Darrieus wind turbine has an axis of rotation perpendicular to the flow of the wind coming in the opposite direction. So, the aerodynamics of this wind turbine presents an aerodynamic behavior unsteady because the angle attack change with the changing of rotation angle of the rotor [1]. Therefore, the main disadvantages of these wind turbines are the high local attack angles and the wake from the blades. The dynamic stall phenomenon has a significant impact on the power of the wind turbine.

The phenomenon of dynamic stall on a blade of the wind rotor is extremely complex, that many effects are combined: three-dimensional effects due to the rotation and finite wingspan of the blades, unsteady effects due to the rotation of the blade and aeroelastic effects due the flexibility of the blades. The study of this type of flow on a rotor in a wind tunnel appears as a challenge in view of the complexity of the aerodynamics of the rotor. Therefore, very few experimental studies of dynamic stall were performed on the bench and very early researchers tried to simplify the experimental conditions.

The literature review shows that studies related to the dynamic effects generated by pale profile movements have largely preceded specific studies of dynamic stall. The analysis of this phenomenon really began very early with the work of Prandtl and the theory of the Prandtl lifting-line [2]. This theory was extended to the case of a moving wing profile thus making it possible to calculate the unsteady lift of the profile. Following the first results of Mc Croskey [3] on the dynamic stall of the oscillating profile, this configuration has been studied and

described by many authors. Various experimental techniques have been implemented to gain a good understanding of the phenomenon of dynamic stall. The most interesting work in this domain has been done by W. Mc. Croskey and Mc. Alister [3,4,5]. The development of computing resources and the need to find new design approaches led the authors to focus their research on the numerical approach using computational Fluid Dynamics (CFD).

A CFD problem modeled with an appropriate turbulence model will give simulation results that are close to physical realities and experimental results.

Using numerical simulation, numerous researches on the aerodynamics of the Darrieus wind turbine has been done recently, we cite the work of Qin et al. [6]. They numerically modeled the flow around the rotor of Darrieus wind turbine. They presented dynamic stall phenomenon and the strong wake interactions of the blades. Castelli M. and Al. [7] performed numerical simulations using the RANS model for VAWT with a rotor with three, four and five blades. They concluded that a reduction in torque is achieved when a vertical axis wind turbine (VAWT) rotates, by increasing the number of blades. Beri, H [8] also investigated the performance of the VAWT with curved profiles and concluded that curved aerodynamic surfaces can make the most of the power of the wind. To improve the prediction in the modeling, particular attention was given to the modeling of the turbulence. Wang and Tao [9] propose a simulation campaign based on complete URANS calculations. They compared the numerical results with the experimental data and they concluded that the two turbulence models SST and k- ε predicted with reasonable precision for low angles of attack. Also, Nobile et al. [10] conducted a 2D study on a three-blade VAWT with NACA0018 profile using different turbulence models, they demonstrated that the SST model gives a better prediction compared to the other models in their analysis. Ferreira et al. [11] note in their work that VAWT exhibits unsteady aerodynamics due to the variation of the attack angle with azimuthal position and relative velocity. For Takamatsu et al. [12],on the contrary, the optimal operating conditions are those where there is no dynamic stall. So many companies and laboratories recently have designed wind turbines with an optimal operating point at reduced speeds high enough so that the dynamic stall does not occur. The study of Fujisawa and Shibuya. [13] showed the disappearance of intense vortices during a dynamic stall. The present work will therefore be structured as follows:

A. Numerical modeling of flow around a profile to explore dynamic stall characteristics for an isolated profile in pitch motion with sinusoidal law. In order to validate our numerical results, comparisons with experimental data will be presented. These results will allow us to make an analysis of dynamic stall phenomenon.

B. A numerical modeling of the flow around a Darrieus rotor with three blades of type H will be carried out in order to predict the dynamic stall of the blade. The URANS approach with the turbulence model k-ω SST will be used. In order to validate our numerical results, comparisons of global coefficients with experimental data will be presented.

2 AERODYNAMICS OF ROTOR H

Figure.1a shows the Darrieus type H wind turbine with three blades. The H-rotor consists of straight blades with an aerodynamic profile. The tower and the arms serve as structural support. When the turbine is subjected to a velocity field perpendicular to its axis of rotation, the blade is therefore subjected to a force parallel to the rotation which generates a torque that rotates the turbine.

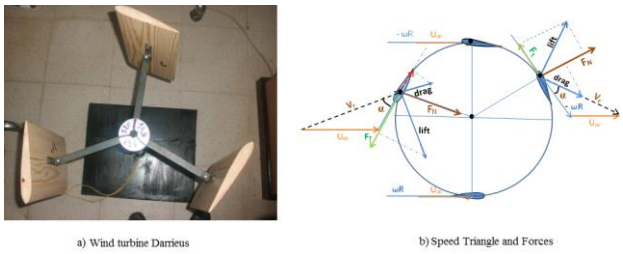

a) Wind turbine Darrieus b) Speed Triangle and Forces

Figure 1. Darrieus Wind Turbine Rotor of FIMA laboratory

The direction and magnitude of the relative velocity changes with the rotation of the blade. The azimuthal angle directly affects the values of the angle of attack, as shown in Figure 1b. The actual maximum and minimum speeds are reached when the blade is at the azimuthal angle 0˚ and 180˚ according to Marco R. Castelli et al. [14].

The attack angle α is the angle between relative wind velocity and the blade rotating direction. [15].

$$\alpha = tang^{-1}\left(\frac{sin\theta}{\lambda+cos\theta}\right) \quad (1)$$

Where λ is the tip speed ratios (TSR) and ϑ is the azimuth angle.

Figure 2 shows the versus azimuth angle at different tip speed ratios. Due to the angle of attack and relative wind speed changes with the azimuth

positions, the forces vary and can be considered as a function of azimuth angle.

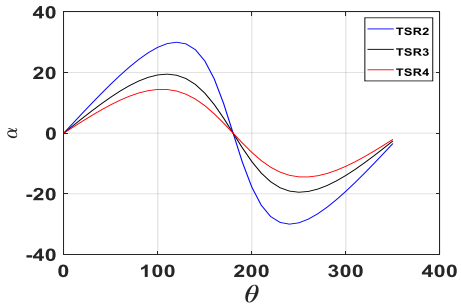

Figure 2: Effective angle of attack versus the azimuth angle at different TSR.

3 METHODOLOGY

The investigations presented in the literature shows us that the studies related to the dynamic effects generated by the blade profile movements largely preceded the specific studies of the dynamic stall for a wind turbine. therefore, in this investigation, we will first present the dynamic stall for a NACA0012 profile in oscillation, then we will extend our investigations for a rotor of a wind turbine Darrieus straight blades in 2D. The two-dimensional approach is adopted to reduce the time and cost of calculation. The rotor analyzed for the VAWT is of type H and its characteristics are listed in Table 1.

3.1 Mathematical Model

The mathematical model includes Continuity and Momentum equations. These equations are solved, with the assumption of incompressible and turbulent-steady flow. Basically, they are the incompressible steady-RANS classical equations. The details of these methodologies are not given here. In RANS, only the time-averaged equations are solved, and the fluctuations associated as Reynolds stresses are represented by turbulence models Continuity and Momentum equations are:

$$\frac{\partial \bar{\rho}}{\partial t}+\frac{\partial(\bar{\rho}\tilde{u}_j)}{\partial x_j}=0 \qquad (2)$$

$$\frac{\partial \bar{\rho}\tilde{u}_i}{\partial t}+\frac{\partial(\bar{\rho}\tilde{u}_i\tilde{u}_j)}{\partial x_j}=-\frac{\partial \bar{p}}{\partial x_i}+\frac{\partial}{\partial x_j}\left(\bar{\tau}_{ij}-\bar{\rho}\widetilde{u_i''v_j''}\right) \quad (3)$$

with

$$-\bar{\rho}\widetilde{u_i''u_j''}=\mu_t\left(S_{IJ}-\frac{2}{3}\frac{\partial \tilde{u}_k''}{\partial x_k}\delta_{ij}\right)-\frac{2}{3}\bar{\rho}k\delta_{ij} \qquad (4)$$

Were μ_t is the turbulent viscosity

To close the system of RANS equations, it is necessary to express the turbulent viscosity μt in function of the mean field, that is to say that it is necessary to have a turbulence model

3.2 Turbulence model K - ω SST

The transport equations for K turbulence energy and ω dissipation of turbulence energy are:

$$\frac{\partial \rho k}{\partial t}+\frac{\partial \rho k u_j}{\partial x_j}=P_K-\beta^{\otimes}\rho\omega K+\frac{\partial}{\partial x_j}\left[(\mu+\sigma_k\mu_t)\frac{\partial k}{\partial x_j}\right] \qquad (5)$$

$$\frac{\partial \rho\omega}{\partial t}+\frac{\partial \rho\omega u_j}{\partial x_j}=\frac{\gamma}{\nu_t}P_K-\beta\ \rho\omega^2+\frac{\partial}{\partial x_j}\left[(\mu+\sigma_\omega\mu_t)\frac{\partial \omega}{\partial x_j}\right]+2\rho(1-F_1)\sigma_\omega\frac{1}{\omega}\frac{\partial k}{\partial x_j}\frac{\partial \omega}{\partial x_j} \qquad (6)$$

The function F_1(Blending function) must take the value 1 near the walls and tend towards zero far away. Menter proposes a function as follows:

$$F_1=tanh\left\{\left\{min\left[max\left(\frac{\sqrt{k}}{B^*\omega y},\frac{500v}{y^2\omega}\right),\frac{4\sigma\omega^2 k}{CD_{k\omega}y^2}\right]\right\}^4\right\} \qquad (7)$$

4 PROFILE MODELIZATION

In our investigation of the flow around the profile, the numerical domain is constituted of a single zone of unstructured mesh. The dimensions of this domain are the following: a height of 10 chords; a length of 20 chords, which 10 of them are upstream of the rotation center of the profile which is at a quarter of the chord and other10 are downstream. The NACA0012 profile is used, in order to obtain numerical results that we will compare with the experimental data of the Mc Alister test cases [4].

Figure 3a represents the mesh of study domain. The movement of the profile in the domain is generated by a dynamic mesh. The unstructured mesh makes it possible to have this mesh, which justified our choice. The resolution of the mesh grid cells were studied and adapted to the morphology of the flow around the profile. We took into account the refinement of the mesh in the zones considered likely to be the seat of a strong gradient of the flow variables. The quality of the grid was checked according to the criterion of the rate of distortion of the elements constituting the mesh. The maximum value of the permissible distortion factor is less than 0.75

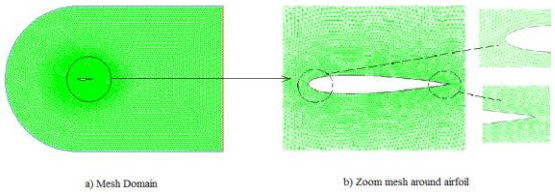

Figure 3: Domain mesh

To obtain the characteristics of the flow in the boundary layer, it is necessary to use a very fine mesh. The mesh is therefore refined close to the wall and is released at the outer boundary of the domain (see Figure 3b). The parameters of the profile movement are the oscillation frequency, the amplitude of the oscillation and the average angle of incidence linked to each other through a law of variation of the sinusoidal angle of incidence such that:

$$a(t) = a_m + A\sin(2\pi ft) \quad (7)$$

With a_m: incidence average angle, A: amplitude of oscillation, f: frequency and t: time. Our choice of the values of the three parameters controlling the flow is identical to the experimental data of the Mc Alister test cases [4]. The incidence average angle is α_m = 15 ° and the amplitude of oscillation is 20 ° inducing a maximum angle of incidence of 25 °. The large amplitude and the maximum angle of incidence cause a deep stall despite a relatively low oscillation frequency. The criterion for the unsteadiness of the oscillating profiles is the reduced frequency dimensioned by the speed of the flow at infinity and the chord of the defined profile:

$$k = \frac{\pi fc}{V_\infty} \quad (8)$$

With c the profile chord and V_∞ the speed upstream. Generally, the unsteady effects are important when k exceeds 0.1, according to Leishman [16]

5 DARRIEUS ROTOR MODELING

The investigation of the flow around the rotor is done in 2D, so the effects of the arms and the support will be neglected. This three-blade rotor is similar to that of the wind turbine test used in the experimental work of Qin et al. [6]

Table 1: Rotor parameters

Designation	Value
Profile	NACA 0021
Rotor diameter	1m
Chord	0.265 m
Angle of inclination	6°

The parameters of this rotor have been accurately recorded and numerated (see Table 1). This numerated geometry of the rotor is used to generate the fluid domains constituting the different areas of computation. In order to minimize the effects of computational domain limits on the simulation results, several numerical tests were performed on the domain dimensions and based on a bibliographic search [9], the values of the geometric parameters selected for our domain in 2D are of a length of 60 R and a width of 30 R, of which R is the radius of the rotor of the VAWT. In order to allow a complete development of the wake, the output of the domain is at 38 R. Figure 4 presents this domain of computation

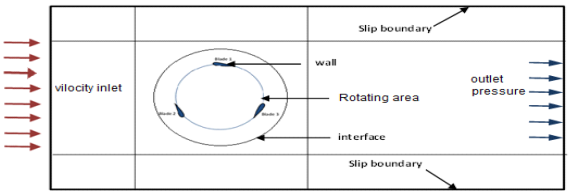

:

Figure4: Computational Domain

To take into account the rotor rotation, the fluid flow domain is divided into two distinct fluid zones: an external fluid domain that represents the wind flow and a rotating domain that represents the rotor of the turbine. Figure 6 illustrates the mesh of the study domain. The moving mesh technique [17] was applied to the rotating domain to predict the overall torque generated by the blades. The outer domain that represents the far field is rectangular. This domain is divided into nine parts in order to use the structured mesh.

The distribution of the mesh grid cells was studied and adapted to the flow morphology of the wind turbine rotor. Two different mesh topologies, structured and unstructured meshes and different mesh resolutions are tested for several time step sizes. To validate the procedure adopted for the mesh of the fluid domains, it is the verification of one of the global parameters such as the torque produced by the rotor.

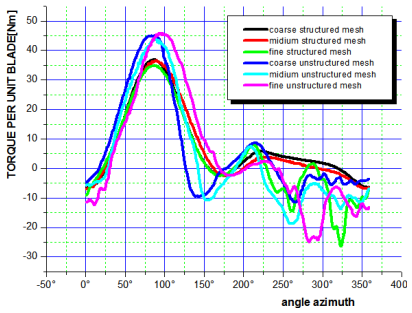

Figure 5. Variation of blade torque with different type of mesh

The Figure 5 shows the results of the blade torque with different type of mesh. The structured mesh gives a better stability of the coefficient of torque produced by the blade; consequently, the structured mesh is adopted in numerical modeling

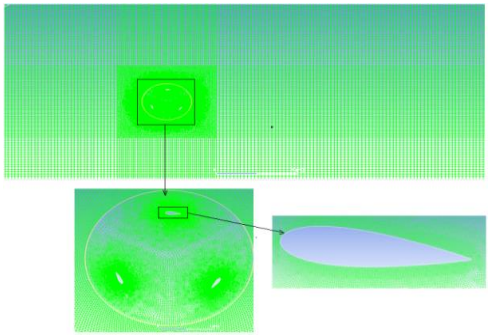

Figure 6. 2D domain mesh

The boundary conditions are defined as follows: The left side limit is defined as the velocity inlet; the right-side limit is defined as the pressure outlet (at atmospheric pressure). A non-slip condition is specified at the blade surface level. The two interfaces of the rotor domain and the external domain are defined as the necessary interface to have a sliding mesh. So that the results of the simulation are not affected by the change of time step and the size of the mesh, several successive tests were conducted for an appropriate choice of mesh. Simulations are performed for different speed ratio (TSR) values between 1.5 and 3.

6 RESULTS AND ANALYSIS

6.1 Dynamic Stall for an isolated profile

The numerical simulations are performed with values of the parameters governing the flow and which are identical to the experimental data of McAlister's and Fisher test. The Authors Mc Croskey and Fisher undertake a program of measure a number of quantities on a wind rotor in test tunnel. These measurements were then compared to analogous measurements made on an oscillating profile.

An analysis of velocity fields obtained on the iso velocity values for six different incidence angles over an entire cycle will be presented. The behavior observed is essentially the same as that of Mc Alister's and Fisher test case. The dynamic stall process is characterized by a sequence of events which is presented in the following figures;

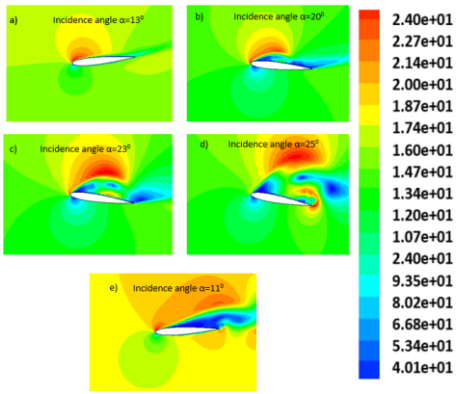

Figure7: Speed fields

Figure 7a shows that for a very small angle of incidence about 13°, the boundary layer is thin without inversion flux, but after that, the impact exceeds the critical angle of attack, an inverted flow layer develops at the trailing edge of the profile.

Figure 7b shows that as the incident angle increases beyond the static stall angle, the flow in the boundary layer begins to reverse on the airfoil. The lift coefficient has further increased for this incidence angle (see Figure 8). Larger vortices begin to form and complete reversal of the flow moves from the trailing edge to the leading edge. When the flow reversal reaches the leading edge, a strong vortex forms at the leading edge.

Figure 7c shows that the vortex continues to roll and grow as it moves towards the back of the blade. This large and intense vortex maintains the curvature of the flow on the bearing surface and prevents the stall. As the vortex moves towards the trailing edge, the curvature of the flow begins to take off and the lift coefficient begins to decrease.

Figure 7d shows that once the leading-edge vortex has been dissipated in the wake, the aerodynamic profile cannot produce anymore the flow curvature required for the generation of the lift. This causes a sudden drop in the lift coefficient. The flow on the bearing surface is completely separated after this point. Consequently, the coefficients of the aerodynamic forces get near their static values. Small eddies continue to form and disappear from the leading edge and the trailing edge, which causes additional instability in charging the pale. This will increase the vibrations of the aeroelasticity and the fatigue of the pale

Figure 7e shows that the boundary layer progressively sticks from the leading edge to the trailing edge with a slower rate and with a delayed manner according to the static case.

The angle of incidence is 11° which is lower than the static stall angle. It is generally necessary to wait until the vortices are transported downstream before the aerodynamic coefficients

reach values comparable to the static case. The evolution of the aerodynamic coefficients during the oscillation of the profile is traditionally represented as a function of the incidence giving the hysteresis cycles for a period of oscillation. The hysteresis cycles are presented in Figure 8.

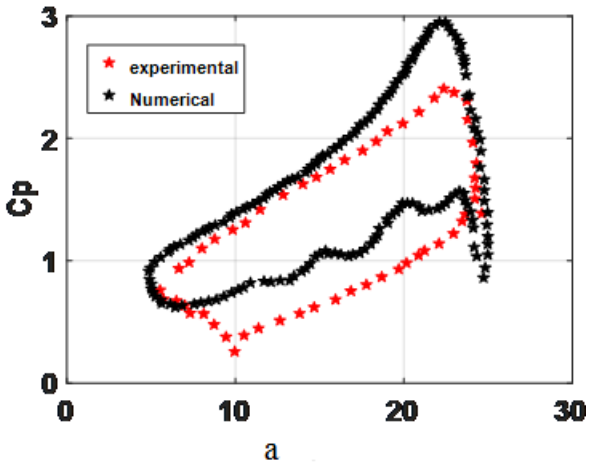

Figure 8: Hysteresis curve of the lift compared to the experimental result

The prediction given by the k-ώ SST model on the development of the vorticity on the whole extrados of the profile which is responsible for the dynamic stall, appears delayed compared to the experimental data. The numerical results overestimate the coefficient of lift for high angles in the ascending part with an error of 10%. Also, these results underestimate this coefficient of lift in the descending part with an error of 10%.

The model k-ώ SST is calibrated according to the hypothesis of a boundary layer without adverse pressure gradient. It underestimates the adverse pressure gradient responsible for the separation of the boundary layer and consequently of the dynamic stall.

The shape of the hysteresis cycle obtained and the angles of incidence for which the profile will pick up during the ascending phase and then hang up during the downward phase are dependent on the effects of the oscillation frequency and the amplitude of the oscillation. The frequency of oscillation and the amplitude of oscillation have a joint effect on the angular rate of variation of incidence.

6.2 Dynamic stall for a Darrieus rotor

When operating a Darrieus wind turbine, the blades are exposed to a variation of incidence angle. For sufficiently small reduced speeds, the incidence angle may exceed the static stall angle on certain parts of their trajectory. Moreover, the rate of change in incidence is generally high, which reunite the conditions necessary for the appearance of dynamic stall. The speed field around the pale is difficult to apprehend, because the wake remains very close to the pale, which makes the influence of the wake on the pale more pronounced. In addition, the pale can cross their own wake, particularly the wake of the upstream phase.

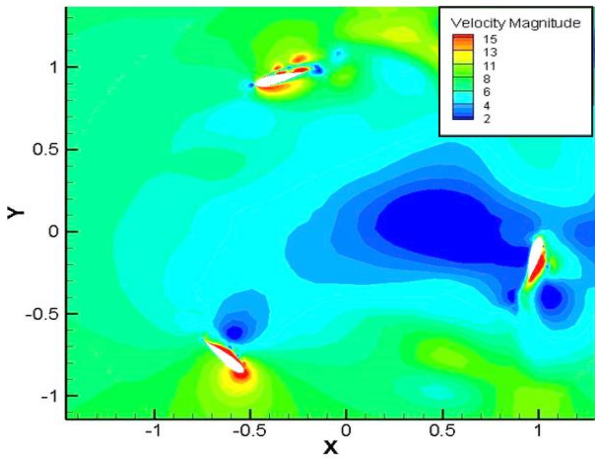

Figure 9: Velocity field around the rotor

Table 2 shows the different azimuthal angles for which stall occurs, according to the TSR. Therefore, the dynamic stall phenomenon depends on the TSR. For a low TSR (λ = 0.5), the dynamic stall occurs at a lower azimuth angle (as TSR increases, dynamic stall occurs at larger azimuth angles.

Table 2. Stall angle according to TSR and azimuthal angle.

TSR	Azimuth Angle (θ	AOF(α)
0.5	38°	22,5°
1	42°	21°
1.75	69°	23°
2.5	92°	22°

The left column of Figure 10 shows the velocity field around the pale before separation of the boundary layer. The right column shows the separation of the flow and vortex formation.

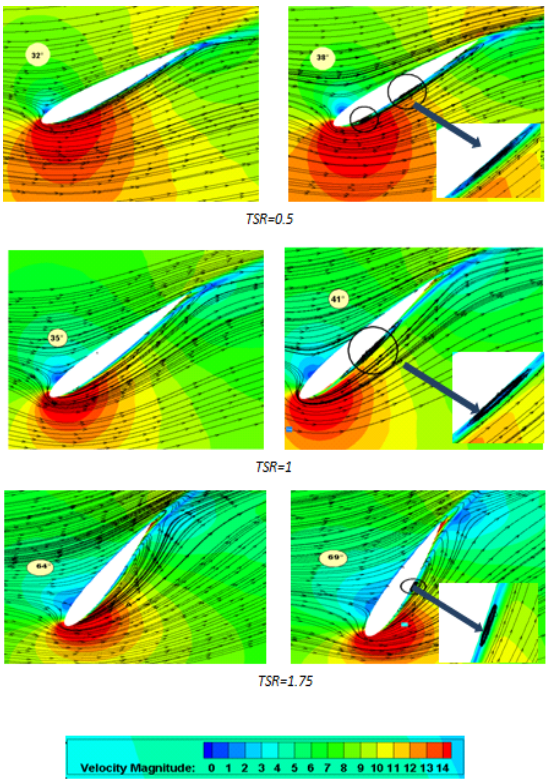

Figure 10. Speed fields for different TSR with azimuth angle

6.3 Average Coefficient torque

The average torque coefficient of a rotor blade was calculated for different TSR. Figure 11 shows the variation of this coefficient as a function of the azimuthal angle for different TSR varying from 0.5 to 3. The maximum value is obtained for an azimuthal angle about 100°. The torque produced by the rotor blade increases upstream until reaching the maximum value, then decreases. This decrease is due to the stall of the flow on the blade.

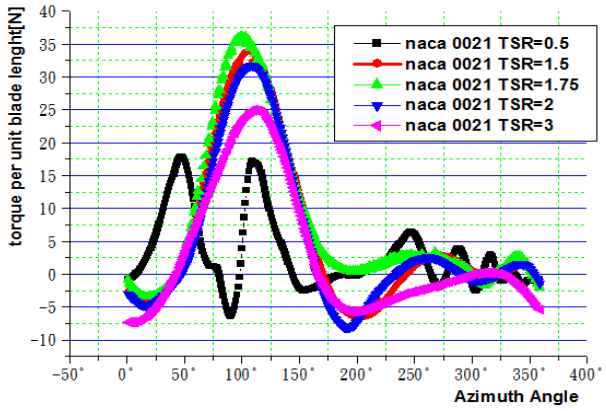

Figure 11: Average torque coefficient

6.4 Comparison and validation

The figure 12 shows the comparison of the power coefficient (CP) variation versus TSR. The numerical results are compared with the experimental data of Qin et al. [4]. Similar trends in the performance curve are obtained from both the experimental data and the numerical modeling. It is also observed, that the power coefficient results of the simulations are overestimated compared to the experimental results for different TSR. These deviations of 8 % in the results are due to several reasons, notably the simplifications adopted in the geometry of the simulation model to the 2D, the neglect of the effect of the arms and the shaft, the phenomenon of numerical diffusion is also a source of error in the numerical simulation of complex flows.

Indeed, a numerical diffusion is assigned to all the numerical resolution schemes of the principal equations, because this last one results from the truncation errors which are a consequence of the writing of the principal equations in a discrete form

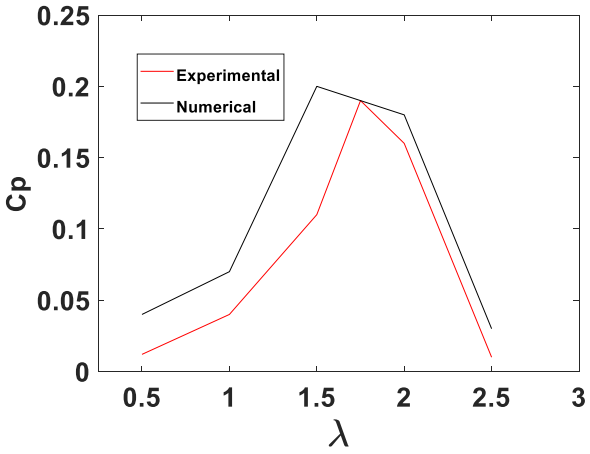

Figure 12: Validation Power coefficient C_P[4]

7 CONCLUSION

This investigation aims for a study of dynamic influence of stall on the aerodynamic performance of a vertical axis wind turbine. The URANS method is used. A very fine mesh has been adopted around the profile and in the wake zone to capture the detachment phenomenon and the formation of vortices of the flow. The investigation of the dynamic stall phenomenon for an oscillating isolated profile gave us a significant result about what would happen in a real rotating blade of a vertical axis wind turbine. Dynamic stall includes the beginning of the flow separation from the blade surface, the complete separation of the boundary layer, the vortex formation and the reattachment of the flow to the airfoil. Dynamic loads could exceed

static values. The flow around an oscillating moving profile is highly unsteady. The shape of the hysteresis cycle obtained and the incidence angles for which the profile will stall during the ascending phase and then to stick during the downward phase depend on the joint effects of the adverse pressure gradient. This is due to the incidence angle and the circulation induced by the movement of the profile. The Two-dimensional modeling of the rotor showed results in agreement with the experiment. The URANS method gave satisfactory results. The pairs predicted by the numerical simulation present a variation according to the attack angle.

We notice that the TSR speed ratio influences the torque and the initiation of flow detachment. The results of the torque produced by the rotor are overestimated. This overestimation in the results is due to the simplifications adopted in the geometry of the simulation model and the phenomenon of numerical diffusion.

Although the dynamic stall increases the performance of the turbine but it causes an increase of the vibrations of the aeroelasticity and the fatigue of the blade.

In summary, the numerical results obtained show that the performance of the blades decreases when the profile is stalled, it is therefore important to design wind turbines operating within the limit of the dynamic stall.

Finally, a better description of the stall phenomenon will help strongly to design and increase the performance of wind turbines.

8 REFERENCES

[1] Yan Chen and Yongsheng Lian “Numerical investigation of vortex dynamics in an H-rotor vertical axis wind turbine” Engineering Applications of Computational Fluid Mechanics, Vol. 9, No. 1, 21 32, (2015).

[2] Ali Memon, “Modèle hybride de surface active pour l’analyse du comportement aérodynamique des rotors éoliens à pâles rigides ou déformables’’. Thèse de doctorat, Arts et Métiers ParisTech, 2009France

[3] M.J. Mc Croskey“Thephenomenon of dynamic stalls NASA technical memorandum” 81264 USA 1981

[4] W. McCroskey, L. Carr, K. McAlister, “Dynamic stall experiments on oscillating airfoils”, *AIAA J*. **14**: 57–63, 1976

[5] W. McCroskey, K. McAlister, L. Carr, S. Pucci, “An experimental study of dynamic stall on advanced airfoil sections. Summary of the experiment”, Vol. **1**. NASA Technical Memorandum 84245, 1982.

[6] Li, Qing'an, Takao Maeda, Yasunari Kamada, Junsuke Murata “Effect of number of blades an aerodynamic force on a straight- blade vertical axis wind turbine”, vol. 90,issue P1, 784-795 (2015).

[7] Marco Raciti Castelli, Stefano De Betta and Ernesto Benini "Effect of Blade Number on a Straight-Bladed Vertical-Axis Darreius Wind Turbine", International Journal of Mechanical, Aerospace, Industrial Mechatronic and Manufacturing Engineering Vol: 6, No:1, (2012).

[8] Beri, H., Yao Y. (2011),"Effect of Camber Airfoil on Self-Starting of Vertical Axis Wind Turbines.’’ J. Environ. Sci. Technol.: 4, p 302 -312.

[9] S. Wang, Z. Tao, “Numerical investigation on dynamic stall associated with low Reynolds number flows over airfoils”, 2nd International Conference on Computer Engineering and Technology (2010).

[10] Nobile1 R., M. Vahdati, J.F. Barlow, A. Mewburn Crook “Unsteady flow simulation of a vertical axis wind turbine: a two-dimensional study”EngD Conference, 2nd. (2013).

[11] Simão Ferreira C. J., A. van Zuijlen, H. Bijl, G. van Bussel and G. van Kuik (2010) “Simulating dynamic stall in a two-dimension a vertical-axis wind turbine: verification andvalidation with particle image velocimetry data Wind Energy”. 2; 13:1–17

[12] Takamatsu et al“A preferable blade profile for high efficiency and the blade characteristics of Darrieus-type cross-flow water turbines”. JSME International Journal, Series II: Fluids engineering, heat transfer, power, combustion, thermophysical properties 34, 2 (1991), 149–156

[13] Fujisawa. N, and Shibuya, S. “Observations wind turbine blades”. Journal of Wind Engineering and Industrial Aerodynamics. 2001

89: p. 201-214.

[14] Marco Raciti Castelli, Stefano De Betta and Ernesto Benini “Effect of Blade Numberon a Straight-Bladed Vertical-Axis Darreius Wind Turbine” ,International Journal of Mechanical, Aerospace, Industrial Mechatronic and Manufacturing Engineering Vol:6, No:1, (2012).

[15] Numerical Investigations of Dynamic Stall ControlFlorin FRUNZULICA, Horia DUMITRESCU2, Alexandru Gheorghe Mihoc-Caius Iacob” 13 Septembrie no. 13, 050711 Bucharest, Romania

[16] J. Leishman, “Dynamic stall experiments on the NACA 23012 Aerofoil, Exp Fluids”, 9(1):49–58, 1990.

[17] Fluent inc. 2002

.

9 NOTATION

N	Numbers of blades [-]
P	Power [Nm / s]
Q	Torque [Nm]
R	Radius of the rotor [m]
C	Power coefficient [-]
R_{ep}	Reynolds Number [-]
U_{∞}	Infinite upstream speed [m / s]

Greek Symbols

$\boldsymbol{\omega}$	Rotational Speed [rad / s]
θ	Azimuth angle [°]
α	Angle of attack [°]
a	Angle of attack of rotor
λ	TSR speed ratio